On the Theoretical Carbon Storage and Carbon Sequestration Potential of Hempcrete

Jay H. Arehart [a], *William S. Nelson*[b], and *Wil V. Srubar III* [a,c,†]

[a] Department of Civil, Environmental, and Architectural Engineering, [b] Department of Chemical and Biological Engineering, [c] Materials Science and Engineering Program, University of Colorado Boulder,

[†] Corresponding Author, T +1 303 492 2621, F +1 303 492 7317, E wsrubar@colorado.edu

Abstract

Hempcrete is a natural insulation material that is well known for exhibiting favorable thermal properties and low manufacturing emissions. Hempcrete is a biocomposite, consisting of hemp shiv and a lime-based binder composed of hydrated lime and either a hydraulic (*e.g.*, natural hydraulic lime and ordinary portland cement) or pozzolanic binder (*e.g.*, metakaolin). While long-term biogenic carbon storage can be achieved *via* utilization of hemp shiv in hempcrete, additional carbon storage can be achieved *via* carbonation of the binder. This study advances previous carbonation modeling approaches by deriving a theoretical model based on the fundamentals of cement hydration and carbonation chemistry to quantify the total theoretical *in situ* CO_2e sequestration potential of hempcrete binders. To estimate the percentage of manufacturing CO_2e emissions that can be recovered through *in situ* binder carbonation, the model is implemented in life cycle assessments of 36 hempcrete formulations of various binder contents and densities using an equivalent functional unit (FU) of a 1m^2 wall assembly with a U-value of 0.27 W/(m^2K). Our model estimates between 18.5% and 38.4% of initial carbon emissions associated with binder production can be sequestered through *in situ* carbonation. Considering biogenic carbon storage, we predict that the total life cycle CO_2e emissions of hempcrete can be negative, with a minimum of -16.0 kg CO_2e/FU for the hempcrete mixture formulations considered herein. However, we estimate that some hempcrete formulations can exhibit net-positive emissions, especially high-density mixes (>300 kg/m^3) containing portland cement, thereby illustrating the importance of materials selection and proportioning in designing carbon-storing hempcrete.

Keywords: hempcrete, carbonation, life cycle assessment, embodied carbon, carbon storage, carbon sequestration.

Highlights:

- A hempcrete carbonation model is derived that considers CO_2 uptake by CH and CSH
- The theoretical model is based on cement hydration and carbonation chemistry
- The model was applied to lime-based, hydraulic, and pozzolanic binders
- CO_2 storage potential of 36 hempcrete mixes were estimated using the model and LCA
- Hempcrete can sequester up to -16 kgCO_2e/m^2 (U = 0.27 W/m^2K) over its lifecycle

1.0 Introduction

Today, the manufacturing of construction materials is responsible for 11% of global greenhouse gas emissions (Adams et al., 2019). To address the climate emergency, curtailment of greenhouse gas emissions in every industry will need to accompanied by large-scale carbon capture and storage strategies (Hansen et al., 2017). Two classes of construction materials possess an inherent ability to store carbon dioxide (CO_2): cementitious materials (e.g., concrete, mortar, and CO_2-derived aggregates), which can sequester carbon *via in situ* carbonation processes, and biogenic materials that store carbon *via* photosynthesis (*i.e.*, wood, bamboo, agricultural products, and other photosynthetic organisms).

Hempcrete, also referred to as hemp-lime concrete or a hemp-lime biocomposite, is a composite construction material that has the ability to store carbon through both carbonation and photosynthesis mechanisms. Hempcrete consists of hemp shiv (*i.e.*, hemp hurd), a byproduct of hemp fiber production, and a lime-based binder. The composition of the lime-based binder varies based upon desired mechanical and physical (*i.e.*, density) properties, but typically consists of hydrated lime with natural hydraulic lime (NHL) or ordinary portland cement (OPC). Hydraulic binders are used with regular hydrated lime to accelerate the set time of hempcrete, as regular limes take weeks to months to gain adequate strength (Magwood, 2016). Pozzolans, such as metakaolin and ground granulated blast furnace slag, have also been used as alternative binders to reduce the global warming potential (GWP) of hempcrete, while preserving its favorable thermal, moisture, and mechanical properties (Walker et al., 2014; Walker and Pavía, 2014).

Hempcrete is primarily used as an insulation material for its low thermal conductivity rather than as a structural or load-bearing material, given its lower strength relative to other construction materials. Two primary construction techniques are used – one, using forms to cast or spray hempcrete directly in place on the construction site and the second, using prefabricated blocks that are transported and installed on-site using methods akin to masonry construction. Hempcrete insulation (in either sprayed or block form) is typically coupled with light-frame timber construction in residential buildings. After mixing,

fresh hempcrete is sprayed (or blocks are laid) between framing members. After installation, finishes and weathering coatings, such as drywall or plasters, are then applied for aesthetics and increased durability.

Previous research has highlighted the potential carbon-negative characteristics of hempcrete (Arrigoni et al., 2017; Boutin et al., 2006; Boutin and Flamin, 2013; Florentin et al., 2017; Ip and Miller, 2012; Nordby and Shea, 2013; Pittau et al., 2018; Pretot et al., 2014). By definition, carbon-negative materials store more carbon dioxide equivalent (CO_2e) than they emit over their life cycle. Life cycle assessments (LCAs) of hempcretes have been conducted to quantify their environmental impacts. Researchers have estimated net life cycle CO_2e emissions of hempcrete from -1.6 to -79 kg CO_2e/m^2 of different wall assemblies (Pretot et al., 2014), depending on (1) functional unit, (2) expected lifetime, (3) LCA methodology (including system boundary assumptions and inclusion or exclusion of biogenic carbon storage), and (4) expected contributions to overall carbon negativity by *in situ* carbonation of cementitious binders beyond cradle-to-gate.

1.1 Carbonation models for hempcrete

To estimate carbon sequestration from *in situ* binder carbonation, LCA practitioners have used manufacturer data (Boutin et al., 2006; Boutin and Flamin, 2013) or mathematical models for quantifying the uptake. Two models have been previously proposed to account for the uptake of CO_2 by the hydraulic binder component of hempcrete. The first (Model A) assumes that only the hydrated lime—or a small fraction of it—carbonates and neglects any carbonation of the hydraulic binder (Florentin et al., 2017; Ip and Miller, 2012; Nordby and Shea, 2013; Pittau et al., 2018). The second (Model B) assumes that all calcium hydroxide, or CH (*i.e.*, portlandite) in cement chemistry notation, in both the hydrated lime and hydraulic binder carbonates (Arrigoni et al., 2017; Pretot et al., 2014). The amount of portlandite (by mass) in hempcrete binders has also been estimated to varying degrees. For example, Pretot *et al.* (2014) assumed that 60% of the hydraulic binder converts to portlandite, while Arrigoni *et al.* (2017) assumed 75% of the calcium-oxide (CaO) present in the hydraulic binder converts to portlandite, as proposed in Lagerblad's work (2006) concerning OPC concrete.

Table 1 summarizes the previous studies that have accounted for CO_2 uptake of cementitious binders in hempcrete. All studies assume through-thickness carbonation within the lifetime of the hempcrete assembly. For the studies that employed Model A, high variation exists in the reported CO_2 uptake from the binder constituent alone (0.091 to 1.19 kg CO_2/kg binder) (Nordby and Shea, 2013; Pittau et al., 2018). Two studies that employed Model B report estimated CO_2 sequestration *via* hempcrete carbonation between 0.325 to 0.462 kg CO_2/kg binder (Arrigoni et al., 2017; Pretot et al., 2014). While Model A is simple to implement, it only captures the aerial carbonation of the hydrated lime. If hydraulic or pozzolanic binders are used, carbonation of the reaction products is not considered leading to an underprediction of hempcrete's ability to sequester CO_2.

In contrast, Model B generally overpredicts hempcrete's ability to sequester CO_2, as it assumes that all CH present in the binder carbonates, neglecting the consumption of CH during additional hydration or pozzolanic reactions. Both Model A and Model B do not consider the effect that pozzolanic reactions have on the amount of CH, nor do they consider the carbonation of calcium-silica-hydrate (CSH), which is also known to decalcify and carbonate in the presence CO_2 (Johannesson and Utgenannt, 2001).

Table 1. Summary of hempcrete LCA studies that estimate and report CO_2 sequestration *via* carbonation. Hempcrete binders comprise up to three components that are reported by their contribution to total binder weight. The CO_2 uptake represent the carbon sequestration which occurs during LCA stages B2 and C, where negative values represent *in situ* carbon sequestration..

Author and Year	Model	Hydrated Lime ratio by weight	Hydraulic Binder ratio by weight	Pozzolanic Binder ratio by weight	CO_2 Uptake in Use (B1) and End of Life (C) (kg CO_2/kg binder)	Reference
Boutin *et al.* 2006	No model specified	Air Lime 0.8	Proprietary Hydraulic binder 0.2	N/A	-0.249	(Boutin et al., 2006)
Ip and Miller 2012	Model A	Hydrated Lime (CL90S) 0.75	Natural Hydraulic Lime (NHL5)	Not specified 0.1	-0.571	(Ip and Miller, 2012)

			0.15			
Nordby and Shea 2013	Model A	Not reported	Not reported	N/A	-0.091	(Nordby and Shea, 2013)
Florentin *et al.* 2017	Model A	Not reported	Not reported	N/A	-0.700	(Florentin et al., 2017)
Pittau *et al.* 2018	Model A	Hydrated Lime (Dolomitic) 0.8	OPC 0.2	N/A	-1.19	(Pittau et al., 2018)
Pretot *et al.* 2013	Model B	Hydrated Lime 0.75	Type I CEM 0.15	Not specified 0.1	-0.462	(Pretot et al., 2014)
Arrigoni *et al.* 2017	Model B	Hydrated Lime (Dolomitic) 0.8	OPC 0.2	N/A	-0.325	(Arrigoni et al., 2017)

1.3 Scope of work

The objective of this work was to derive a simple, yet comprehensive, mathematical model based on lime and cement hydration and carbonation chemistry for quantifying the theoretical carbon storage potential of hempcrete. The model is subsequently implemented in a LCA of a 1 m^2 hempcrete wall assembly with a constant U-value of 0.27 W/(m^2K) to estimate the net life cycle CO_2e emissions of hempcrete and to specifically highlight the potential contribution of *in situ* carbonation to overall carbon storage potential. **Section 2** describes the theoretical formulation of the model, as well as the goal and scope of the LCA. **Section 3** presents the results of the LCA, which employs three different carbonation models (*i.e.*, Model A, Model B, and the model proposed herein). In addition, **Section 3** illustrates how using different models to predict *in situ* carbonation can influence the total GWP calculation of hempcrete.

2.0 Computational Methods

2.1 Theoretical Formulation

The theoretical mass of CO_2 that can be stored by hempcrete wall assemblies *via in situ* carbonation is quantified using principles of cement chemistry. This section first describes the chemical composition of the binders and estimates the total quantities of expected hydration reaction products (*i.e.*, CH and CSH). The anticipated reduction of the total amount of portlandite available for carbonation due to the

conversion of portlandite to CSH in the presence of siliceous pozzolans is mathematically accounted for in the model formulation. Lastly, the stoichiometry of carbonation reactions between atmospheric CO_2 and hydration products is used to estimate the theoretical mass of CO_2 that is sequestered *via* carbonation of the hempcrete binders.

2.1.1 Hempcrete binder chemistry

Binders for hempcrete construction consist primarily of three constituents: hydrated lime, hydraulic binders, and pozzolanic binders. **Table 2** summarizes the average chemical and mineral composition of the binders used in hempcrete construction.

Hydrated lime, also known as slaked lime, is composed of 80-90% pure CH. Referred to as *aerial lime*, hydrated lime hardens and gains strength by reacting directly with CO_2. To accelerate the time aerial limes take to gain strength, hydraulic binders and pozzolanic binders are used in combination with aerial lime to increase early-age mechanical properties of hempcrete. Common hydraulic binders for hempcrete include Type I OPC and natural hydraulic lime (NHL). When OPC and NHL are exposed to water, they react to form portlandite (*i.e.*, CH). However, pozzolanic binders, such as metakaolin, require both water and a source of CH to produce CSH, which also increases the mechanical properties of cementitious materials (Magwood, 2016). Therefore, pozzolanic binders are almost always used in combination with hydraulic binders.

Type I OPC is composed mainly of silicon dioxide (S), aluminum oxide (A), ferric oxide (F), calcium dioxide (C), magnesium oxide (M), sulfur trioxide (Š), and sodium oxide (N). These oxides are the building blocks of four main cementitious minerals present in OPC: tricalcium silicate (C_3S), dicalcium silicate (C_2S), tricalcium aluminate (C_3A), and tetracalcium aluminoferrite (C_4AF). NHL only consists of C_2S as its primary form of silicates. In addition to C_2S, NHL also contains some hydrated lime. NHL is similar to hydrated lime in that it is primarily composed of portlandite (*i.e.,* CH). NHL is classified into three types based upon its intended use; NHL 2, NHL 3.5, and NHL 5.

Table 2. Average chemical and mineral compositions of hempcrete binder components (by wt.%).

	Chemical	Hydrated Lime (CL90-S)	Type 1 Ordinary Portland Cement	Natural Hydraulic Lime (NHL 5)	Metakaolin
Chemical Composition	C (CaO)	65-75	63.9	50-70	0.07
	S (SiO_2)	-	20.5	6-20	52.1
	A (Al_2O_3)	-	5.4	-	41.0
	F (Fe_2O_3)	-	2.6	-	4.32
	M (MgO)	-	2.1	-	-
	Š (SO_3)	-	3.0	-	-
	N (Na_2O)	-	0.61	-	-
	Other	25-35	1.9	15-20	-
	Source	(Chabannes et al., 2018)	(ASTM C150, 2019)	(Chabannes et al., 2018)	(Wild and Khatib, 1997)
Mineral Composition					
	CH	80-90	-	30-50	-
	C_2S	-	18	20-40	-
	C_3S	-	54	-	-
	C_3A	-	10	-	-
	C_4AF	-	8	-	-
	Cč ($CaCO_3$)	5-10	-	5-20	-
	Other	0-5	10	0-15	100
	Source	(Chabannes et al., 2018)	(ASTM C150, 2019)	(Chabannes et al., 2018)	(Badogiannis, et al., 2005)

Metakaolin is a common pozzolanic additive composed primarily of three oxides: S, A, and small amounts of F (Khatib, et al., 1997). Metakaolin is a pozzolan that is produced from calcining kaolinite clay at high temperatures. Metakaolin can be used to replace cementitious materials due to its pozzolanic activity when combined with hydraulic binders, such as OPC or NHL.

2.1.2 Hydration Reactions

While hydrated lime (~80-90% CH) can directly carbonate with atmospheric CO_2, hydraulic binders must first undergo cement hydration reactions to produce CH. The primary hydration reactions of the calcium silicate minerals with water produce CH and CSH, shown in Eqs. 1-4 (Mehta, 1986). When NHL, which consists of only C_2S as a mineral form of calcium and silica, is used as a binder in hempcrete, the only hydration reaction that occurs is shown in Eq. 1, the hydration of C_2S. When OPC is used as a binder, all four hydration reactions occur due to the presence of all minerals in Type I cement:

$$2C_2S + 9H \rightarrow C_3S_2H_8 + CH \quad (1)$$

$$2C_3S + 11H \rightarrow C_3S_2H_8 + 3CH \quad (2)$$

$$C_4AF + 2CH + 14H \rightarrow C_6(A,F)H_{13} + (F,A)H_3 \quad (3)$$

$$C_3A + 3C\check{S}H_2 + 26H \rightarrow C_6A\check{S}_3H_{32} \quad (4)$$

In cement chemistry (*i.e.*, oxide) notation, water is denoted as H, gypsum as $3C\check{S}H_2$, ettringite as $C_6A\check{S}H_{32}$, calcium aluminoferrite hydrate as $C_6(A,F)H_{13}$, and aluminoferrite hydrate as $(F,A)H_3$.

2.1.3 Pozzolanic Reactions

In addition to the hydration reactions, the presence of pozzolans leads to the production of CSH. Siliceous and aluminous materials from SCMs, such as metakaolin, react with available CH, effectively decreasing the amount of CH available for carbonation, as shown by Eqs. 5-6 (Mehta, 1986):

$$3CH + 2S + 5H \rightarrow C_3S_2H_8 \quad (5)$$

$$3CH + A + 3H \rightarrow C_3AH_6 \quad (6)$$

However, the pozzolanic reaction involving aluminum oxide is not typically considered, as silicates are the main reactive component within most pozzolans (Dunstan, 2011; Souto-Martinez et al., 2017). Therefore, reaction (Eq. 6) is neglected in the proposed model.

2.1.4 Carbonation Reactions

The carbonation of hempcrete refers to the process in which atmospheric carbon dioxide (CO_2) reacts with the binder (*i.e.*, CH and CSH). In general, the carbonation of CH consumes CO_2 and precipitates calcium carbonate ($CaCO_3$), as described in Eq. 7:

$$Ca(OH)_{2(aq)} + CO_2 \rightarrow CaCO_{3(s)} + H_2O_{(l)} \quad (7)$$

The carbonation of CSH also occurs in lime-based binders according to Eq. 8, assuming that CSH takes the simplified form of: $CSH = 3Ca(OH)_2 + SiO_2$ (Johannesson and Utgenannt, 2001).

$$3Ca(OH)_{2(aq)} + SiO_{2(s)} + 3CO_2 \rightarrow 3CaCO_{3(s)} + SiO_2 + 3H_2O_{(l)} \quad (8)$$

Several other trace compounds in cement paste, such as magnesium oxide (Olajire, 2013) and ferric oxide phases (Das et al., 2014), have also been known to undergo carbonation reactions. For the proposed

model, however, these reactions are neglected, as they are less significant than the primary carbonation reactions and their mechanisms and extents of reaction in cement paste have not been as thoroughly investigated. Note that the assumption of ignoring these phases will result in a more conservative estimate for the overall CO_2 storage potential of hempcrete *via in situ* carbonation.

2.2 Carbonation Model

From the hydration and pozzolanic reactions, the theoretical quantity of CO_2 that is sequestered by a specific hempcrete mixture can be calculated according to Eqs. 9a-9c:

$$\mathrm{C_{m,CH}} = \alpha_{\mathrm{CH}} - \beta_{\mathrm{CH}} \tag{9a}$$

$$\mathrm{C_{m,CSH}} = \alpha_{\mathrm{CSH}} + \beta_{\mathrm{CSH}} \tag{9b}$$

$$\mathrm{C_m} = \mathrm{C_{m,CH}} + \mathrm{C_{m,CSH}} = (\alpha_{\mathrm{CH}} + \alpha_{\mathrm{CSH}}) - (\beta_{\mathrm{CH}} - \beta_{\mathrm{CSH}}) \tag{9c}$$

where $C_{m,CH}$ and $C_{m,CSH}$ are the total mass quantities of CO_2 that are sequestered by CH and CSH, respectively, in units of kg CO_2/kg of binder paste. α_{CH} and α_{CSH} are the CO_2 storage potential based upon the quantity of CH or CSH, respectively, after the completion of the carbonation (in units of kg CO_2/kg carbonated binder paste). β_{CH} and β_{CSH} are the CO_2 storage potential based upon the quantity of CH or CSH, respectively, after the completion of the pozzolanic and carbonation reactions (in units of kg CO_2/kg carbonated binder paste).

2.2.1 Carbon storage potential of the hydraulic binder and hydrated lime

The carbon storage potentials of the hydraulic binder and hydrated lime are represented by the variables α_{CH} and α_{CSH}, respectively. These variables are computed from the ratio of mineral consumption in the hydration reactions to the CO_2 consumption in the carbonation process scaled by their molecular weights (Eqs. 10 and 11):

$$\alpha_{\mathrm{CH}} = \left[\phi_{\mathrm{h}}\left(\frac{3}{2}\frac{\mathrm{K_{C_3S}}}{\mathrm{MW_{C_3S}}} + \frac{1}{2}\frac{\mathrm{K_{C_2S}}}{\mathrm{MW_{C_2S}}} - \frac{2}{1}\frac{\mathrm{K_{C_4AF}}}{\mathrm{MW_{C_4AF}}}\right) + \frac{\mathrm{K_{CH}}}{\mathrm{MW_{CH}}}\right] * \mathrm{MW_{CO_2}} \tag{10}$$

$$\alpha_{\mathrm{CSH}} = 3 * \left[\phi_{\mathrm{h}}\left(\frac{1}{2}\frac{\mathrm{K_{C_3S}}}{\mathrm{MW_{C_3S}}} + \frac{1}{2}\frac{\mathrm{K_{C_2S}}}{\mathrm{MW_{C_2S}}}\right)\right] * \mathrm{MW_{CO_2}} \tag{11}$$

where ϕ_h is the degree of hydration, K_{C_3S}, K_{C_2S}, K_{C_4AF}, and K_{CH} are concentrations (in decimal form) of C_3S, C_2S, C_4AF, and CH, respectively, and MW_{C_3S}, MW_{C_2S}, MW_{C_4AF}, and MW_{CH} are the molecular weights of C_3S (228.31 g/mol), C_2S (172.24 g/mol), C_4AF (242.98 g/mol) and CH (74.09 g/mol), respectively. The coefficients are stoichiometric ratios derived from Eqs. 1-8 of the CH and CSH produced during the hydration of the hydraulic binder, or initially present in the hydrated lime, to the total estimated quantity of either CH or CSH produced by the hydration reaction. The negative coefficient for C_4AF represents the consumption of CH during hydration, as mathematically described by Eq. 3.

2.2.2 Carbon storage potential of the pozzolanic binder

With the addition of pozzolanic binders, the available CH is consumed and converted to CSH (Eq. 5). Both CH and CSH carbonate and the total mass of CO_2 consumed during this reaction is represented by β_{CH} and β_{CSH}. These two quantities are computed depending upon which reactant is limiting. To determine which reactant is limiting, the ratio of Eq. 12 should be used:

$$Q = \frac{S}{\alpha_{CH} * \frac{MW_{CH}}{MW_{CO_2}}} \tag{12}$$

If Q = 0, then there are no silicates (S) present and Eq. 13a is used to compute β_{CH} and β_{CSH}. If $Q \geq 0.5406$, then CH is the limiting reactant and Eq. 13b is used to compute β_{CH} and β_{CSH}. If $Q < 0.5406$, then S is the limiting reactant, and Eq. 13c calculates the correct values for β_{CH} and β_{CSH}. The value of 0.5406 (g CO_2/g binder) is determined by the stoichiometry and molar ratio of the conversion of CH to CSH to CO_2 denoted by both the pozzolanic and carbonation reaction equations.

$$\beta_{CH} = 0,\ \beta_{CSH} = 0 \tag{13a}$$

$$\beta_{CH} = \alpha_{CH},\ \beta_{CSH} = 0.594 * \alpha_{CH} * \frac{MW_{CH}}{MW_{CO_2}} \tag{13b}$$

$$\beta_{CH} = 1.099 K_S,\ \beta_{CSH} = 1.099\ K_S \tag{13c}$$

When no pozzolans are present in the system (Eq. 13a), $\beta_{CH} = 0$ and $\beta_{CSH} = 0$, as expected. Depending upon the silica (S) content of the pozzolan, either CH or S will be the limiting reagent within the pozzolanic reactions (Eqs. 5-6). If CH is limiting (Eq. 13b), then $\beta_{CH} = \alpha_{CH}$ and $\beta_{CSH} = 0.594 * \alpha_{CH} *$

$\frac{MW_{CH}}{MW_{CO_2}}$, where α_{CH} is calculated from Eq. 9. If S is limiting (Eq. 13c), then it is assumed that all of the available silica is converted to CH and CSH, thus $\beta_{CH} = 1.099\ K_S$ and $\beta_{CSH} = 1.099\ K_S$, where K_S is the concentration of S. The scalar of 1.099 is determined by calculating the molar ratio of CH or CSH to silica (3 to 2) from Eq. 5, dividing the ratio by the molecular weight of SiO_2 (60.08 g/mol) and multiplying by the molecular weight of CO_2 (44.01 g/mol) (Souto-Martinez et al., 2017). Typically, if a pozzolanic binder is used, it is used in small enough quantities such that CH is the limiting reactant and Eq. 13c is employed to calculate the necessary coefficients β_{CH} and β_{CSH}.

2.2.3 Total carbon storage potential of hempcrete binders

C_m, described by Eq. 8c, represents the total CO_2 uptake in kg per kg of hydrated binder in a hempcrete mixture. To evaluate the carbon storage potential of hempcrete, C_S, a *mass* factor, θ, defined herein as a mass ratio of hydrated binder paste to hempcrete, is required. In addition, since not 100% of the CH or CSH will carbonate (Despotou et al., 2016), a *carbonation* factor, ϕ_C, is required.

Eq. 14a provides the calculation for the total carbon storage potential of the binder per unit mass of hempcrete, while the contributions of CH and CSH carbonation are detailed by Eqs. 14b and 14c, respectively.

$$C_s = \phi_C * C_m * \theta \quad (14a)$$

$$C_{s,CH} = \phi_C * C_{m,CH} * \theta \quad (14b)$$

$$C_{s,CSH} = \phi_C * C_{m,CSH} * \theta \quad (14c)$$

The proposed model assumes that the entire volume of a hempcrete assembly undergoes the same degree of carbonation within its lifespan. Experimental evidence has informed this assumption. Previous research has shown that after 240 days of exposure at ambient conditions, the volume of carbonated hempcrete varies with depth, being close to zero below a depth of 6 cm (Arrigoni et al., 2017), while under one month of accelerated carbonation, a bulk rate of carbonation of 66.7% can be achieved throughout the entire assembly (Chabannes et al., 2015). Based upon this accelerated carbonation experimental evidence, the model assumes that, over the anticipated service life of hempcrete (~60-100 years), that sufficient

carbonation will occur throughout the full depth of the assembly. Additional long-term experimental data on the *rate* of carbon uptake in hempcrete at ambient conditions would provide additional support for this assumption.

Studies of historic structures built with lime mortars has shown that carbonation processes halt after a degree of carbonation of 86% is obtained for thin, exposed mortars, and 75% for thick, covered mortars (Despotou et al., 2016). Thus, while degree of carbonation is ultimately up to the discretion of the modeler, it is recommended that a degree of carbonation of 75% be used as an input for the model proposed herein ($\phi_C = 0.75$).

2.3 Carbonation Model Implementation in Hempcrete LCA

2.3.1 Mix Designs

The theoretical carbonation model derived in the previous section was implemented in life cycle assessments (LCAs) of 36 theoretical hempcrete mixture designs (see **Table 3**). These mixtures represent conventional hempcrete mixtures. Binders consist of different combinations of hydrated lime (CL90 – S) and three types of hydraulic binders, NHL, (OPC), and MK. Each binder combination is used to evaluate the model at three different concentrations of hydraulic or pozzolanic binder: low (20%), medium (35%), and high (50%), and at three different densities: very light (175 kg/m^3), light (225 kg/m^3), medium (300 kg/m^3), and high (425 kg/m^3), based upon common ranges for residential construction in North America (Magwood, 2016). Each density of hempcrete is the result of different hemp-to-binder-to-water ratios (by mass) (see **Table 4**).

Table 3. Representative hempcrete mixture design formulations.

Mix Number	Mix Name	Block Density	Density (kg/m^3)	Binder Types	Binder Paste by Volume Percent (Decimal)			
					HL (CL90 - S)	NHL 5	OPC Type 1	Metakaolin
1	NHL+High+VL	Very Light	175	HL and NHL	0.500	0.500	-	-
2	NHL+Mid+VL	Very Light	175	HL and NHL	0.650	0.350	-	-

3	NHL+Low+VL	Very Light	175	HL and NHL	0.800	0.200	-	-
4	OPC+High+VL	Very Light	175	HL and OPC	0.750	-	0.250	-
5	OPC+Mid+VL	Very Light	175	HL and OPC	0.825	-	0.175	-
6	OPC+Low+VL	Very Light	175	HL and OPC	0.900	-	0.100	-
7	MK+High+VL	Very Light	175	HL and Metakaolin	0.500	-	-	0.500
8	MK+Mid+VL	Very Light	175	HL and Metakaolin	0.550	-	-	0.450
9	ML+Low+VL	Very Light	175	HL and Metakaolin	0.600	-	-	0.400
10	NHL+High+L	Light	225	HL and NHL	0.500	0.500	-	-
11	NHL+Mid+L	Light	225	HL and NHL	0.650	0.350	-	-
12	NHL+Low+L	Light	225	HL and NHL	0.800	0.200	-	-
13	OPC+High+L	Light	225	HL and OPC	0.750	-	0.250	-
14	OPC+Mid+L	Light	225	HL and OPC	0.825	-	0.175	-
15	OPC+Low+L	Light	225	HL and OPC	0.900	-	0.100	-
16	MK+High+L	Light	225	HL and Metakaolin	0.500	-	-	0.500
17	MK+Mid+L	Light	225	HL and Metakaolin	0.550	-	-	0.450
18	MK+Low+L	Light	225	HL and Metakaolin	0.600	-	-	0.400
19	NHL+High+M	Medium	300	HL and NHL	0.500	0.500	-	-
20	NHL+Mid+M	Medium	300	HL and NHL	0.650	0.350	-	-
21	NHL+Low+M	Medium	300	HL and NHL	0.800	0.200	-	-
22	OPC+High+M	Medium	300	HL and OPC	0.750	-	0.250	-
23	OPC+Mid+M	Medium	300	HL and OPC	0.825	-	0.175	-
24	OPC+Low+M	Medium	300	HL and OPC	0.900	-	0.100	-
25	MK+High+M	Medium	300	HL and Metakaolin	0.500	-	-	0.500
26	MK+Mid+M	Medium	300	HL and Metakaolin	0.550	-	-	0.450
27	MK+Low+M	Medium	300	HL and Metakaolin	0.600	-	-	0.400
28	NHL+High+H	Heavy	425	HL and NHL	0.500	0.500	-	-
29	NHL+Mid+H	Heavy	425	HL and NHL	0.650	0.350	-	-
30	NHL+Low+H	Heavy	425	HL and NHL	0.800	0.200	-	-
31	OPC+High+H	Heavy	425	HL and OPC	0.750	-	0.250	-
32	OPC+Mid+H	Heavy	425	HL and OPC	0.825	-	0.175	-
33	OPC+Low+H	Heavy	425	HL and OPC	0.900	-	0.100	-
34	MK+High+H	Heavy	425	HL and Metakaolin	0.500	-	-	0.500
35	MK+Mid+H	Heavy	425	HL and Metakaolin	0.550	-	-	0.450
36	MK+Low+H	Heavy	425	HL and Metakaolin	0.600	-	-	0.400

Table 4. Hemp-to-binder-to-water ratios for different mixture densities (adapted from Magwood (2016)).

Hempcrete Density	Parts Hemp	Parts Binder	Parts Water
Very Light	1	1	1.5
Light	1	1.25	1.75
Medium	1	1.75	1.75
Heavy	1	2.5	2.25

2.4 LCA Methodology

2.3.2 LCA Goal and Scope

Using the ISO 14040/14044 framework (ISO, 2006a, 2006b), LCAs are performed to quantify the total global warming potential (GWP) of a functional unit of hempcrete. The goal of the LCA is to implement the proposed carbonation model to understand the total carbon storage potential of hempcrete, which will be useful to building product manufacturers and building designers for use in in whole-building LCA.

The functional unit considered in this LCA is 1 m^2 of non-load-bearing insulation made with hempcrete cast on-site between temporary formwork. The target insulation application requires an insulation layer that achieves a heat transfer coefficient of 0.27 W/(m^2K) (R-20). This U-value was selected to represent target thermal insulation levels specified by US residential building codes in cold climates (IECC, 2017). Thickness and, thus, total volume, of the functional unit will vary for each hempcrete mixture formulated in **Table 3**. While the thermal conductivity of hempcrete varies by binder type and moisture content, the simplified empirical relationship (Eq. 15) proposed by Collet and Pretot (2014) for both precast and sprayed assemblies relates λ is thermal conductivity (mW/(mK)) to density, ρ (kg/m^3), of hempcrete.

$$\lambda = 0.4228 * \rho - 42.281 \quad (15)$$

Eq. 15 was used to calculate the thickness of each functional unit. The corresponding volume of the functional unit is calculated by multiplying the thickness (m) by 1 m^2. Because the thermal conductivity

of hempcrete assembly is dependent upon the density, different mix designs result in different sized functional units. The functional unit geometries are summarized in **Table 5**.

Table 5. Thickness and total volume of 1 m^2 hempcrete insulation (U-value = 0.27 W/(m^2K)).

Hempcrete	Density	Computed Thermal Conductivity (W/(mK))	Required Thickness (m)	Total Volume of Functional Unit (m^3)
Very Light	175	0.032	0.12	0.12
Light	225	0.053	0.20	0.20
Medium	300	0.085	0.31	0.31
Heavy	425	0.137	0.51	0.51

The system boundary of the LCA includes stages A1-A3 (product, or "cradle-to-gate" stage) and B1 (use-stage) as defined by EN 15804 (EN, 2011). The product stage includes the material extraction (A1) (including biogenic carbon storage), transportation (A2), and manufacturing (A3) for both the binder and the hemp shiv. The use stage (only B1) includes the carbonation of the binder and neglects all other maintenance or repair stages. End-of-life stages (C1-C4) are ignored due to the assumption that full carbonation is achieved during the lifespan of the hempcrete assembly. Construction stages (A4-A5) and other use stages (B2-B7) are not included in the analysis because they are assumed to be equivalent across all mix designs considered and thus do not support the goal of the LCA. The only environmental impact considered by the assessment is 100-year global warming potential (GWP), measured in kg of carbon-dioxide equivalent (kg CO_2e), due to its immediate importance to keep global average temperatures from increasing more than 1.5°C (UNFCCC, 2015).

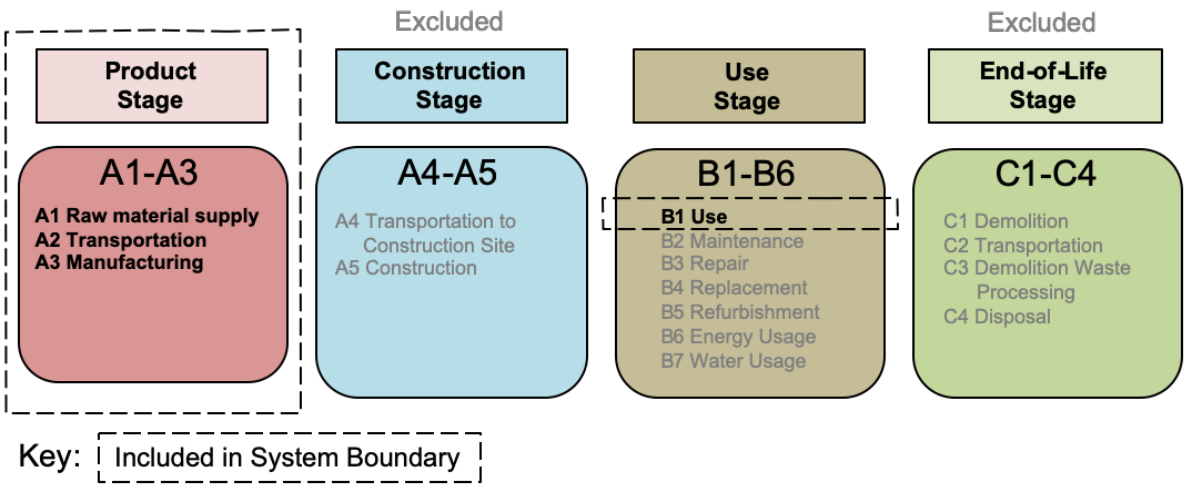

Figure 1. System boundary of the hempcrete LCA. Life cycle stages A1-A3 represent material extraction and manufacturing emissions (including biogenic carbon storage), while use-phase (B1) represents the carbon uptake *via* carbonation.

2.3.3 Life cycle Inventory (LCI) Data

Life cycle inventory (LCI) data were collected from peer-reviewed literature and open-source datasets for each material constituent in the hempcrete formulations. The environmental impacts are attributional and are allocated on a per-mass basis. **Table 6** summarizes the data collected, its source, quality, and suitability for this LCA. Data for hydrated lime is given "medium" reliability, given its publication date of 2010 and the fuel type of the lime kiln having a significant impact on the cradle-to-gate emissions. The rest of the data are considered to have high reliability, given that it is timely data obtained from peer reviewed LCA publications. It is assumed that data collected for specific manufacturing processes are representative of the average emissions for worldwide production. While different hemp growing practices and manufacturing processes will affect total emissions from life cycle stages A1-A3, the carbonation model presented herein could still be used to predict the carbon storage potential of hempcrete due to binder carbonation in LCA Stage B1.

This LCA assumes that biogenic carbon is stored by the hempcrete assembly for the duration of the lifespan and that the hempcrete crop is replaced within a year of harvest. Additionally, since hemp is

mixed with a binder, it is not expected to decompose at the end-of-life. These assumptions simplify the need for dynamic LCA, and biogenic carbon can be counted as a benefit to the GWP of the hempcrete assembly in LCA Stage A1.

Table 6. LCI data for the GWP of a declared unit of each hempcrete material constituent. Note that emissions for hemp shiv are separated into manufacturing emissions (positive value) and biogenic uptake (negative value).

Material	A1 - A3 GWP (kg CO_2e/kg material)	Reliability	Source and Comments
Hydrated Lime	1.2	Medium	Efficient lime production from 2010 study on a lime-producing plant. (Ochoa George et al., 2010)
NHL 5	0.635	High	Peer-reviewed data for Europe NHL5 production (Grist et al., 2015)
Type 1 OPC	0.912	High	UK specific Inventory of Carbon and Energy v3.0 (Jones and Hammond, 2019)
Metakaolin	0.421	High	Peer-reviewed study for metakaolin production allocated by mass (Heath et al., 2014)
Hemp Shiv (Emissions)	0.104	High	Timely peer-reviewed study for Italian hemp production allocated by mass (Zampori et al., 2013)
Hemp Shiv (Biogenic Uptake)	-1.84	High	Timely peer-reviewed study for Italian hemp production allocated by mass (Zampori et al., 2013)
Water	0.003	High	US-specific LCA in accordance with ISO14044 (Franklin Associates, 2009)

2.4 Limitations of the Study

- While the chemical and morphological diversity of CSH is high (Morandeau et al., 2014; Wu and Ye, 2016), it is assumed that CSH takes the primary form of $C_3S_2H_8$. If the calcium-to-silicon ratio (C/S) ratio decreases over time, as it is well known to do during carbonation (Nonat, 2004), the actual stoichiometric ratios in the carbonation reaction will change, affecting the coefficients of α_{CSH} and the overall estimate carbon storage results. However, the estimate for carbon storage potential *via* carbonation remains conservative, given that the calcium that would become available for additional carbonation during CSH destabilization and decalcification during carbonation is not accounted for in

the model.

- Experimental validation of the carbonation model is outside the scope of this study. Since the model is chemistry-based (using stoichiometry), and there is ample existing research on the carbonation of other cementitious materials, this study focuses on the model's value of prediction and the consequences of choosing different models to predict carbonation on the overall LCA results.
- As a screening LCA, only life cycle stages A1-A3 and B1 were considered as part of the system boundary to elucidate the results between different mix designs. Additionally, the environmental impacts associated with LCA stages A4 (transportation to site) and A5 (construction) were assumed equivalent for each mix design and not considered in the LCA. Inclusion of these stages within the system boundary could, however, change the results.
- Biogenic CO_2 storage is best modeled using dynamic LCA (Breton et al., 2018) and will produce different results compared to the simplified screening LCA methodology used herein (Levasseur et al., 2013). While giving more accurate results, the use of dynamic LCA did not directly support the goal of the study, which was to illustrate the implementation of a new, theoretical carbonation model for hempcrete to calculate carbon storage potential in the context of total life cycle carbon emissions. However, the model presented herein can be adapted for implementation in dynamic LCA.
- Full, through-thickness carbonation during the lifetime of the hempcrete assembly is assumed in this LCA. This assumption is informed by experimental studies, as previously described. In other words, the service lifetime is assumed sufficient for the carbonation front to move from the surface through the thickness of the hempcrete. In addition, we assume that 75% of all cement paste in the hempcrete that is exposed to CO_2 actually carbonates—an assumption that was also informed by previous studies. The depth, rate, and degree of carbonation is dependent upon many factors, such as humidity, CO_2 concentration, binder paste density, and time. While Arrigoni *et al.* experimentally showed that no carbonation below a depth of 6 cm was achieved after 240 days of exposure. Due to the long lifespan of buildings (60-100 years), full through-thickness carbonation of assemblies is anticipated.

3.0 Results and Discussion

3.1 CO_2 Storage Potential via Carbonation

3.1.1 Effect of binder type

Using the proposed carbonation model, the estimated *in situ* carbon sequestration potential of hempcrete mixtures for each concentration of hydraulic or pozzolanic binder (High, Mid, and Low) is shown in **Figure 2**. Carbonation is separated into CH and CSH carbonation to represent the mass of CO_2 per mass of binder that is stored during the carbonation process. The more hydrated lime that is available (low hydraulic or pozzolanic additive concentration), the higher the total carbon uptake across all mixtures. For mixtures with hydraulic binders (NHL and OPC), for example, the carbon uptake through CH carbonation dominates the carbon uptake through the carbonation of CSH. For example, as shown in **Figure 2**, the NHL+Mid mixtures have an estimated carbonation potential of 0.47 kg CO_2/kg binder, where 0.43 kg CO_2/kg binder is achieved *via* carbonation of CH and 0.04 kg CO_2/kg binder is achieved *via* carbonation of CSH. Additionally, as less hydraulic binder is used, less CSH is produced and, therefore, less CSH is available to carbonate. Contrastingly, more CH is available from the slaked lime, thereby increasing the carbonation potential. Due to OPC containing more silica than NHL, much of the available calcium oxides (*i.e.*, C_2S and C_3S) are converted not only to CH but also to CSH (see Eqs. 1 and 2), which results in a higher carbon uptake from CSH carbonation, as expected. Mixes that utilize NHL as a hydraulic binder correspond to the highest carbonation potential due to the highest amounts of calcium oxide available.

In comparison to mixtures with hydraulic binders, mixtures with metakaolin (a pozzolan) exhibit much lower carbonation potentials per mass of binder, as expected. In these mixtures, CH is consumed in pozzolanic reactions (Eqs. 5 and 6), which results in no CH available for carbonation. Therefore, total carbonation potential equals the total theoretical uptake by CSH alone. As observed for the hydraulic binder mixtures, as the concentration of metakaolin decreases, the total carbon uptake decreases. At the low concentrations of pozzolanic additive, more hydrated lime is present in the mixture that is converted to CSH, which is subsequently available to carbonate. If silica (S) is the limiting reagent, some CH would

be unconsumed after the pozzolanic reactions, which would result in some CH carbonation. High concentrations of pozzolanic mixtures would elucidate this result, yet these proportions are not conventionally used in residential hempcrete construction.

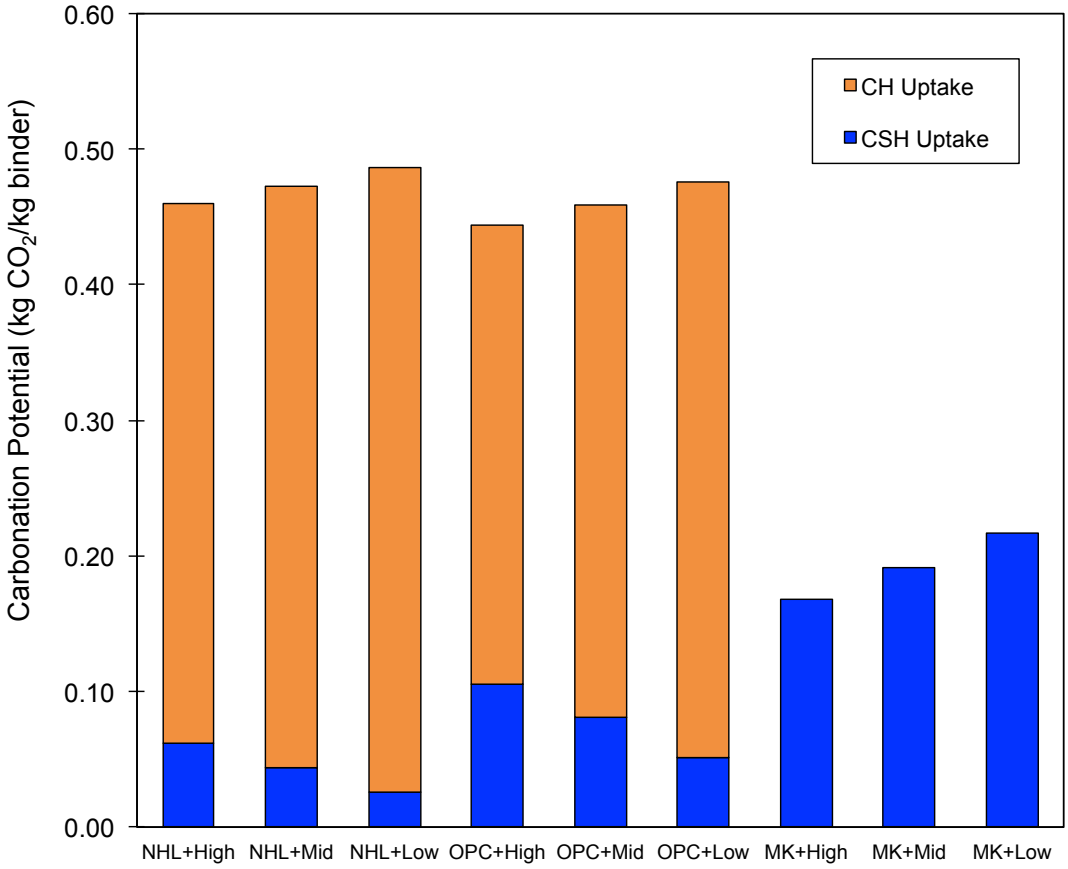

Figure 2. Effect of binder composition on the theoretical CO_2 storage potential (per mass of binder) for all densities of hempcrete mixtures.

3.1.1 Effect of density

The target density of a hempcrete mixture influences the total amount of binder. **Figure 3** compares the theoretical carbon uptake *via* carbonation (B1) per functional unit of different hempcrete mixtures across different target densities. Note that the carbon storage potential in **Figure 3** is represented by positive (rather than negative) values. As expected, higher-density mixtures exhibit higher propensities for carbon

uptake *via* carbonation due to the higher amounts of binder required to create the functional unit. For example, functionally equivalent very light, light, medium, and heavy NHL mixes with medium concentration of hydraulic binders have binder masses of 5.87 kg, 13.76 kg, 36.54 kg, and 94.04 kg, respectively, corresponding to estimated carbon uptake *via* carbonation of 2.1 kg CO_2, 4.9 CO_2, 12.9 CO_2, and 33.3 CO_2, respectively.

These results, as well as those presented in **Figure 2**, illustrate that the theoretical carbon storage potential of hempcrete *via in situ* carbonation is proportional to the mass of binder, as anticipated. Thus, increasing the mass of the binder (*i.e.*, higher-density mixtures) increases the total estimated carbon uptake *via* carbonation. Heavy density mixtures contain ~10 times the mass of binder compared to very light mixtures, which results in higher carbon sequestration potential estimates per functional unit.

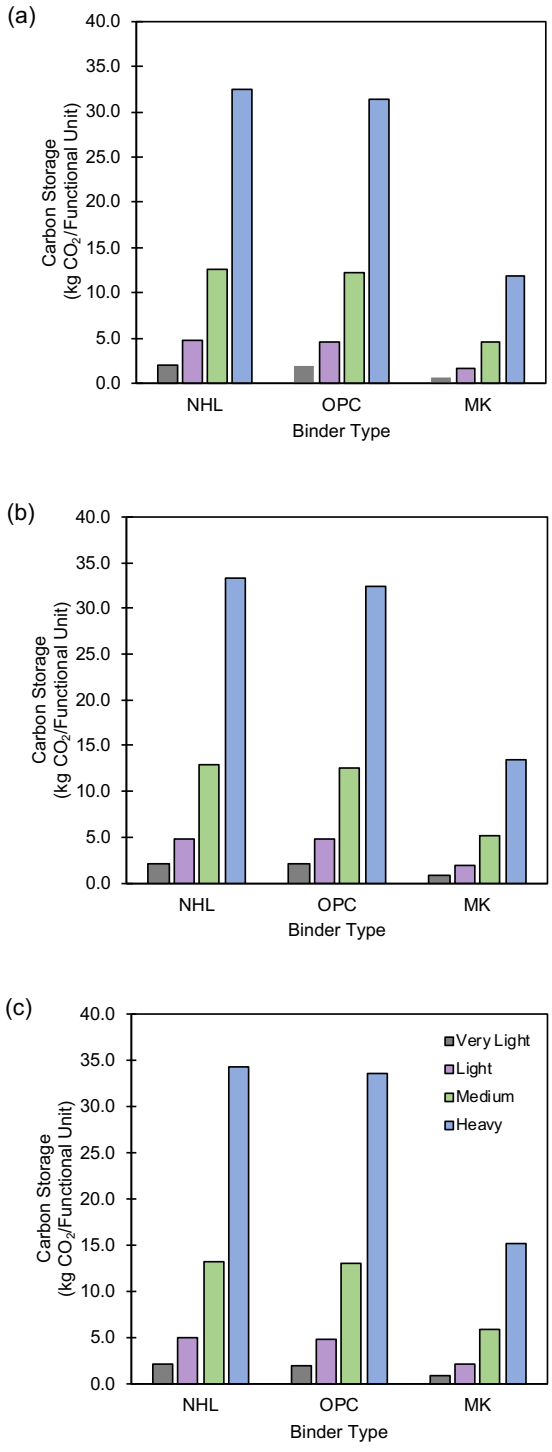

Figure 3. Effect of hempcrete density on the theoretical carbon uptake of hempcrete *via* carbonation for three different hydraulic binder concentrations (a) high, (b) mid, and (c) low.

3.1.3 Comparison of carbonation models

The two models identified in the literature (Model A and Model B), along with the model proposed herein (Model C), were used to estimate the theoretical carbon uptake *via* carbonation of all mix designs in **Figure 4**. As previously discussed, Model A only considers carbonation of the hydrated lime, while Model B considers the carbonation of all CH. Model C considers carbonation of the avilable CH and CSH from a cement and carbonation chemistry perspecitve and accounts for the use of multiple binders and pozzolanic additives.

As evidenced by the comparative estimates in **Figure 4**, Model B provides higher estmates of the carbon storage potential of hempcrete *via* carbonation as compared to Model A and Model C for mixtures containing NHL and OPC. For example, for the medium density, high-concentration NHL mixture (mix number 19), Models A, B, and C predict carbon storage of 8.5 kg CO_2/FU, 13.7 kg CO_2/FU, and 12.6 kg CO_2/FU respectively. For the high-concentration NHL mixtures, Model A provides lower estimates of CO_2 uptake *via* carbonation compared to Model C, since it does not consider the presence of calcium oxides in the hydaulic binder. Model B provides higher estimates of CO_2 uptake compared to Model C, since it assumes 75% of all availabe CaO converts to CH, neglecting the formation of CSH and its associated carbonation potential. The tendancy for Model B to provide higher estimates of CO_2 is most evident for the mixtures containing OPC (**Figure 4b, 4e, 4h, and 4k**). Since OPC contains more silicates, it produces more CSH than mixtures with NHL. For the medium density, high-concentration OPC mix (mix number 22), Model B predicts a carbon uptake through carbonation of 23.0 kg CO_2/FU as compared to the 12.2 kg CO_2/FU prediction of Model C—an increase of ~ 90%. The difference between these two models illustrates how different models for carbonation can lead to different results.

For mixtures with MK, Model A and Model B provide higher estimates of carbon uptake compared to Model C. For the medium density, low-MK mixture (mix number 27), Model A predicts 7.0 kg CO_2/FU, Model B predicts 5.9 kg CO_2/FU, and Model C predicts 5.2 kg CO_2/FU. Due to the precence of pozzolans (a source of silica), Model C accounts for hydrated lime that is fully consumed to produce CSH. Models A and B neglect formation of CSH, which results in higher estimates of carbon uptake.

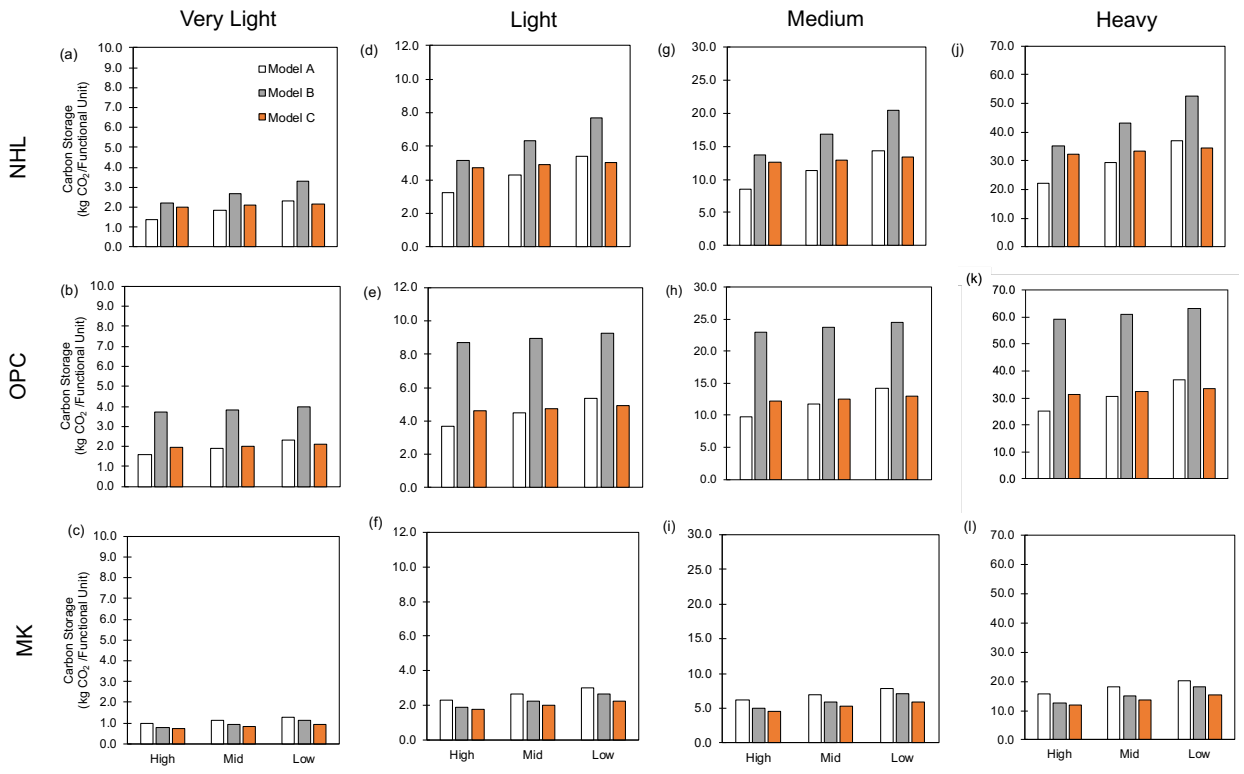

Figure 4. Comparison of carbonation models on theoretical estimates of carbon uptake *via* carbonation of different hempcrete formulations: **(a)** - **(c)** Very Light, **(d)** – **(f)** Light, **(g)** – **(i)** Medium, and **(j)** – **(l)** Heavy densities.

3.2 LCA Results

CO_2 uptake *via* binder carbonation (Stage B1) is only one component of the life cycle emissions of a hempcrete assembly. **Figure 5** illustrates the carbon storage potential of hempcretes in relation to total life cycle emissions for hydraulic and pozzolan binder hempcrete mixtures for different densities. The vertical axis represents the GWP ($kgCO_2e$) per functional unit, where negative values correspond to carbon storage and positive values correspond to carbon emissions. For each mixture, the processes associated with carbon emissions are plotted on the left (A1-A3), and storage (both biogenic and carbonation) on the right. The net difference between the left and right columns is an estimate of total life-cycle emissions. For example, in **Figure 5a**, the heavy density mixtures (NHL+H) has two columns, emissions on the left and storage on the right. The emissions are associated with hemp, binder, and water production, totaling

to 105.09 kg CO_2e. The carbon storage through both carbonation and biogenic uptake is -103.46 kg CO_2e. Thus, the net emissions of the NHL+Low+H mixture (Mix 30) are positive (indicating Mix 30 is a net CO_2 emitter), of 1.63 kg CO_2e and are represented by the bottom of the right bar. If the bottom of the right column is below zero, the hempcrete functional unit has negative net-emissions. If it is above zero, the hempcrete functional unit has positive net-emissions.

As anticipated, initial CO_2 emissions are dominated by binder production. Hemp production contributes small quantities of cradle-to-gate emissions, as measured and reported by Zampori *et al.* (Zampori et al., 2013). Emissions associated with water use are negligible (<0.55% of total emissions). Binder manufacturing contributes represents the largest contributor to the life cycle emissions as a result of the calcination process required to produce hydrated lime and hydraulic binders. Across all mixture types, increasing density increases binder mass and, thus, emissions associated with manufacture. MK-containing mixtures (**Figure 5g, 5h, and 5i**) exhibit lower emissions from the binder, since the manufacturing process for metakaolin is less energy and emissions intensive. However, as explored previously, the carbon uptake through carbonation for the mixtures with metakaolin is lower than those with hydraulic binders.

The results illustrate that 18.5-38.4% of initial emissions from binder production can be recovered through the carbonation process. However, high carbonation potential of the binder does not necessarily correspond to the mix design with the most carbon storage per functional unit. For NHL (**Figure 5a, 5b, and 5c**), the medium density, high-concentration mix design (Mix 19) exhibits the lowest total carbon emissions, -15.95 kg CO_2e/FU, as compared to the other NHL mixtures. However, that mix has -12.60 kg CO_2/FU of carbon stored through carbonation, which is significantly less than the high-concentration NHL heavy density mixture (Mix 28), which has an estimated carbon uptake through carbonation of –32.42 kg CO_2/FU. This finding is similar to previous work by the authors, which showed significant carbon uptake—but overall higher net carbon emissions—of OPC concrete and pervious concrete mixtures with high cement contents (Ellingboe et al., 2019; Souto-Martinez et al., 2018).

The amount of biogenic carbon stored for each mix design is shown in **Figure 5**.The amount of hemp shiv in each mix is directly proportional to the target mix density. Hence, when the biogenic carbon coefficient of -1.84 kg CO_2/kg hemp shiv (Zampori et al., 2013) is applied, the amount of carbon stored increases.

Nearly all mix designs result in net carbon storage during their life cycle. The mix designs that maximize carbon storage of the hempcrete assembly are the NHL+High+M (Mix 19), MK+High+M (Mix 25), and MK+Mid+M (Mix 26) mixtures with a life cycle GWP of -15.95 kg CO_2e/FU, -15.86 kg CO_2e/FU, and -15.19 kg CO_2e/FU respectively. Nearly all MK-based mixtures outperform their hydraulic binder counterparts due to the carbon intensity of manufacturing hydraulic binders.

While hempcrete is often deemed a carbon-negative material, not all mix designs considered herein result in net storage. The heavy density (425 kg/m^3) low-concentration OPC-containing mixtures, for example, showed a positive GWP (8.16 kg CO_2e/FU) after all storage components were considered. Heavy density mixtures are often considered for semi-structural applications, yet, depending on the mixture design, the hempcrete assembly may not store carbon and another functionally equivalent insulation material may have lower carbon emissions.

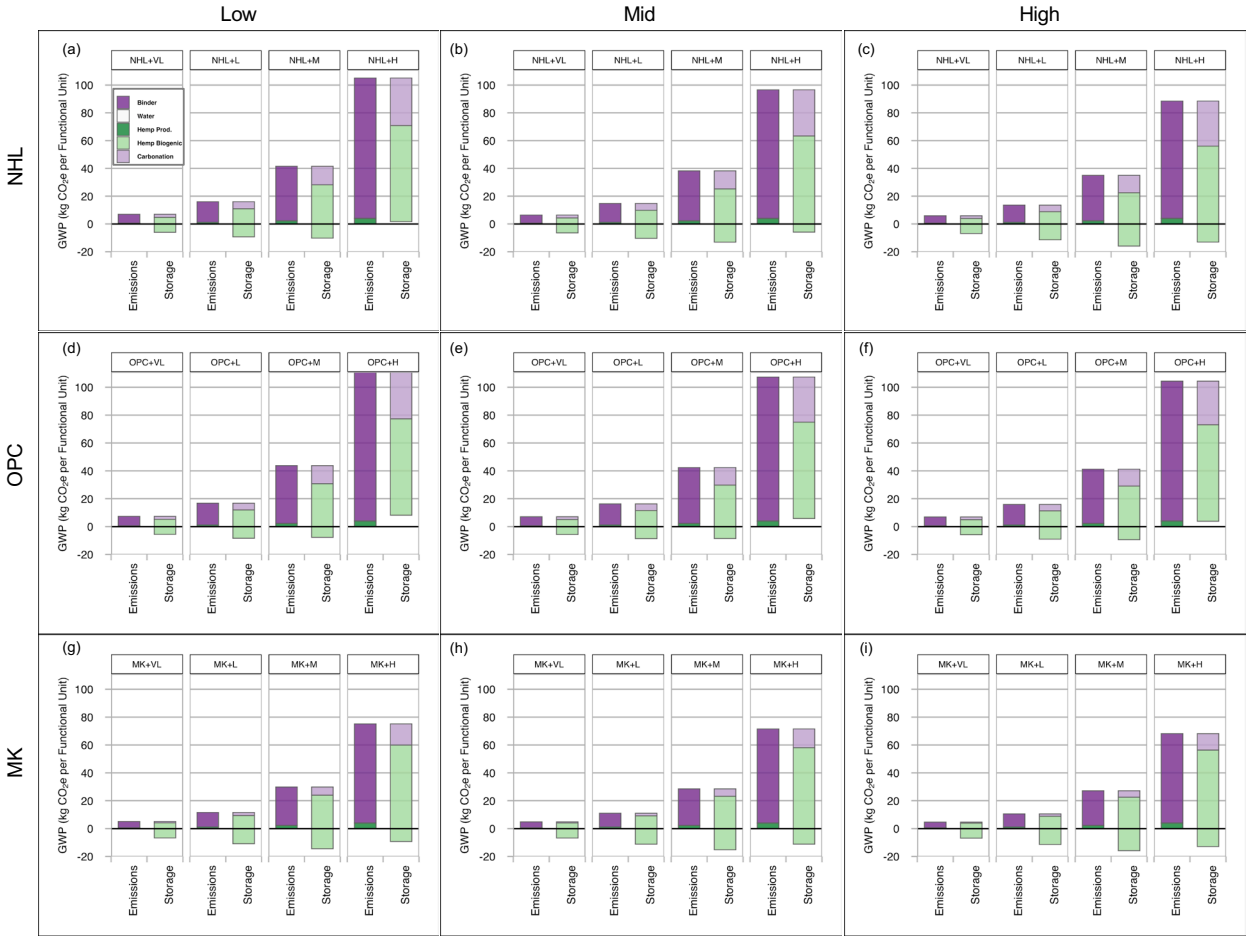

Figure 5. Life cycle GWP ($kgCO_2e$) for each hempcrete mixture of hydraulic and pozzolanic binders: (**a**) – (**c**) natural hydraulic lime, (**d**) – (**f**) ordinary portland cement, and (**g**) – (**i**) metakaolin.

3.4 Effect of Carbonation Model Selection on LCA Results

Each of the carbonation models that have been proposed in the literature (Model A and Model B) and the model proposed herein (Model C) are implemented to evaluate how model choice impacts LCA results. **Figure 6** and **Figure 7** present the life cycle emissions calculated with each model for the mid-concentration, medium density NHL mix design (Mix 20) and the mid concentration, medium density MK mix design (Mix 26), respectively. For the selected NHL mix design, the total GWP ranges from -11.56 kg CO_2e/FU (Model A), -17.00 kg CO_2e/FU (Model B), and -13.15 kg CO_2e/FU (Model C). A

manifestation of the results observed in **Figure 4**, Model A and Model B provide more and less conservative estimates of total emissions in comparison to Model C, respectively.

For the MK mix design (see **Figure 7**), both Model A (GWP = -16.94 kg CO_2e/FU) and Model B (GWP = -15.84 kg CO_2e/FU) provide higher estimates of total carbon storage potential compared to Model C (GWP = -15.19 kg CO_2e/FU). This result is attributable to the pozzolanic reactions that are accounted for in Model C (Eq. 5 and Eq. 6), which are not considered by either Model A or Model B. The differences in life cycle GWP as calculated by different carbonation models highlights the importance of model choice, since not accounting for the pozzolanic reactions provides an overestimation of the carbon storage potential of hempcrete.

As opposed to other carbonation models, the hempcrete carbonation model described in this study (Model C) accounts for all hydration and pozzolanic binder reactions in addition to the carbonation of both CH and CSH. The model can be applied to hempcrete mix designs of various densities and binder constituents, including pozzolans, for which previous models did not account. While most mix designs show net-negative carbon emissions (net storage), mix designs with high densities show positive life cycle emissions.

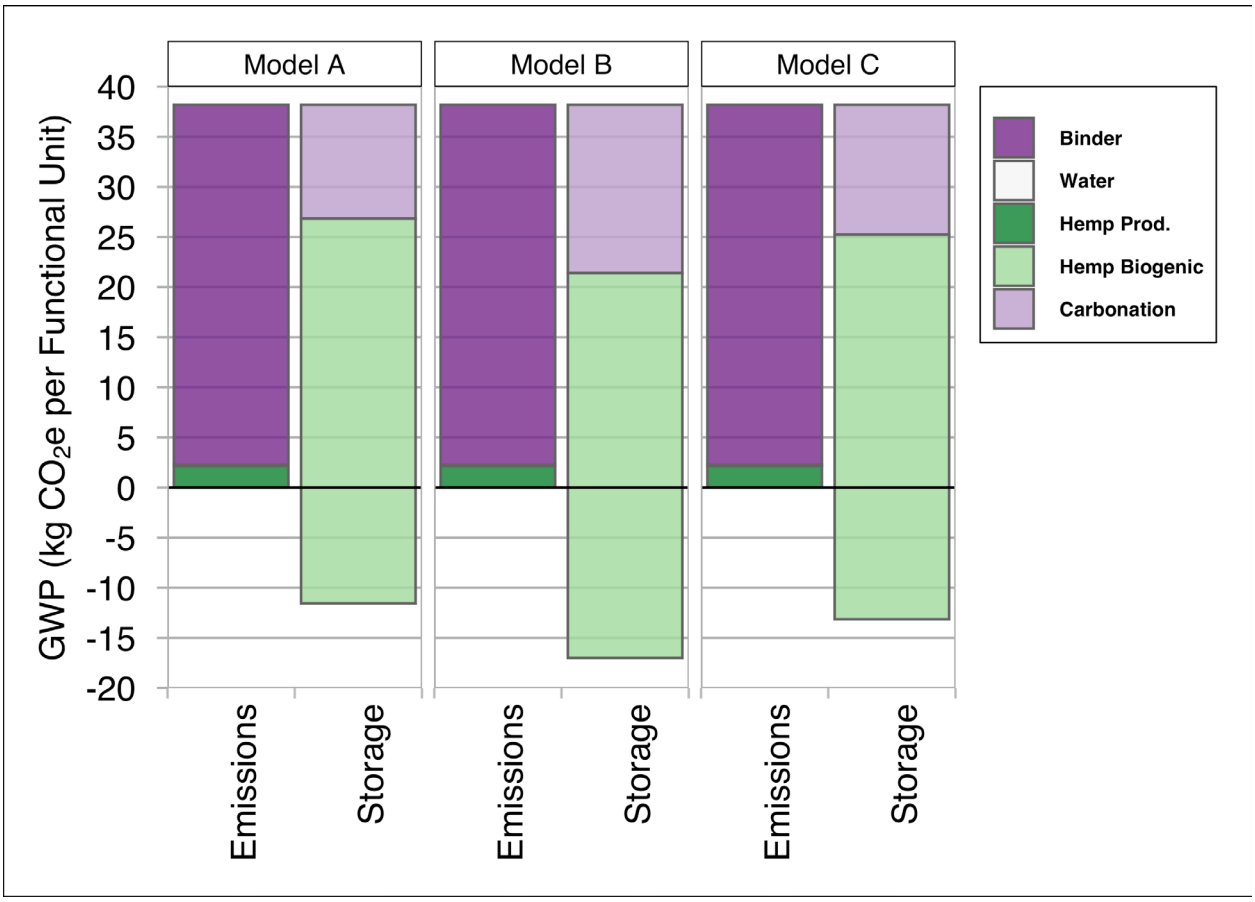

Figure 6. Effect of carbonation model on LCA results for GWP medium density natural hydraulic lime with mid concentration of hydraulic binder (Mix 20).

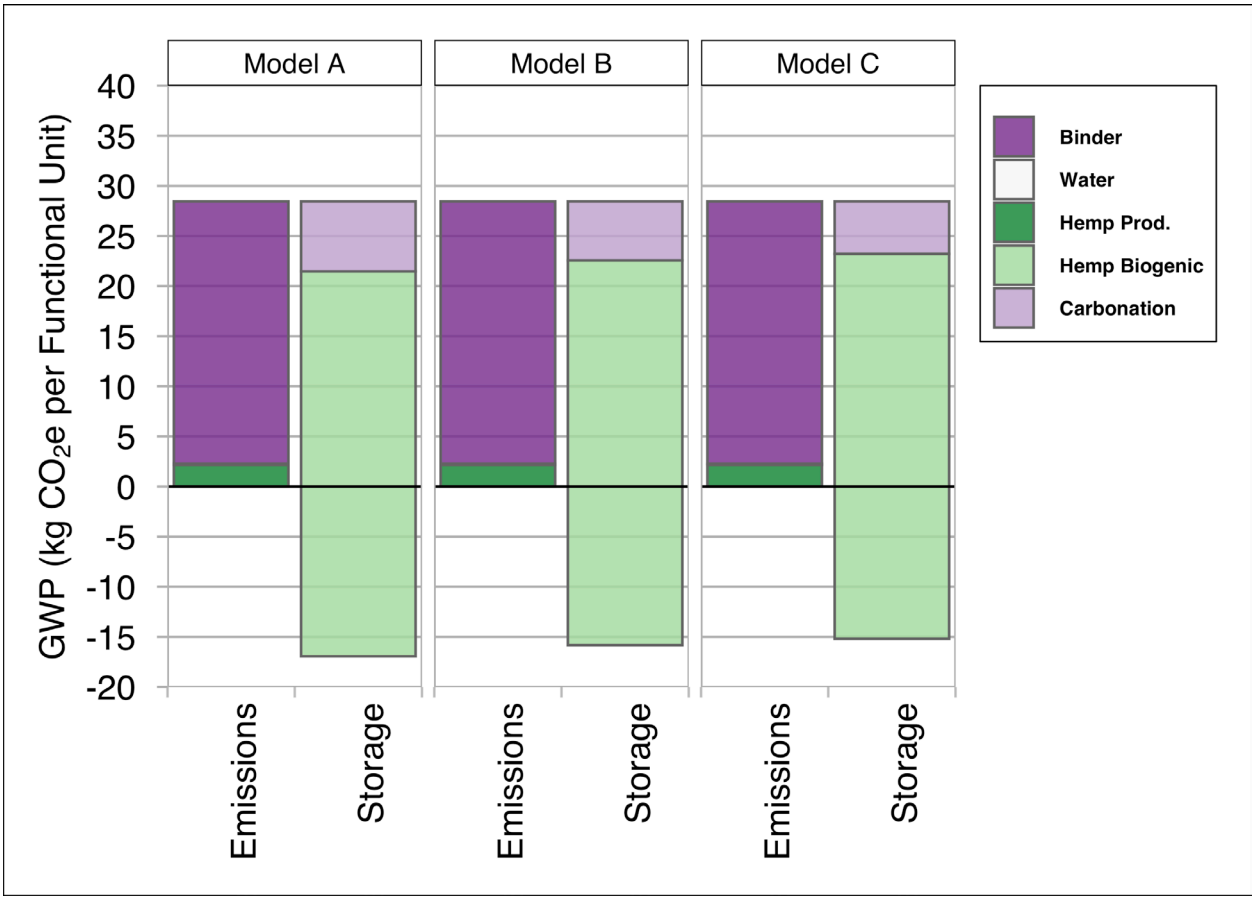

Figure 7. Effect of carbonation model on LCA results for GWP medium density natural hydraulic lime with mid concentration of hydraulic binder (Mix 26).

4.0 Conclusions and Future Prospects

To better predict the carbon storage potential of hempcrete, the formulation and implementation of a mathematical model based on the stoichiometry of hydration, pozzolanic, and carbonation reactions was presented herein. The model was implemented in a screening LCA of 36 hempcrete mixture design to quantify the life cycle GWP of a functional unit (1 m^2 of wall with a U-value of 0.27 W/(m^2K)).

Key findings from this study include:

- The more calcium oxide present in the binder before hydration, the higher the carbonation potential on a per-mass-of-binder basis. However, maximizing carbonation potential does not necessarily correspond to maximizing total carbon storage of a functional unit of hempcrete.

- The carbonation model formulated herein estimates between 18.5% to 38.4% of initial emissions from binder production can be sequestered through the carbonation process. When biogenic carbon storage is also considered, net emissions of -13.15 kg CO_2e/m^2 are predicted when hydraulic binders are use (mid-concentration, medium density NHL mixture) and net emissions of -15.84 kg CO_2e/m^2 when pozzolanic binders are used (mid-concentration, medium density metakaolin mixture). Mix designs that use metakaolin (a pozzolan), while not maximizing carbon storage *via* carbonation, minimizes total life cycle GWP and carbon storage due to lower initial emissions associated with binder production.
- High-density mixtures (425 kg/m^3), often used for their higher strengths, do not maximize carbon storage. In fact, when OPC is used as a hydraulic binder in high-density mixtures, results illustrate that hempcrete assemblies could be a net CO_2 emitter (up to 8.16 kg CO_2e/FU).

The model formulated and implemented in this study confirms that many hempcrete mixture designs exhibit net-negative carbon emissions (*i.e.*, carbon storage). The results suggest that low-density, natural hydraulic binder mixtures are key to maximizing the carbon-storage potential of hempcrete. This work also illustrates how the chemistry-based carbonation model can be used in combination with LCA to estimate the carbon-storage potential of hempcrete in achieving low-carbon building design objectives.

Based upon the results presented herein, a number of new research questions have been elucidated. Long-term, experimental quantification of the real-time carbonation potential of *in situ* hempcrete assemblies would provide validation to the model's ability to quantify carbon storage. Furthermore, experimental evidence on the rate of carbonation of hempcrete assemblies with different mixture designs will provide additional insight into the speed of carbon uptake. Since the application of modern hempcrete assemblies is relatively nascent, long-term durability experiments and case studies will provide much needed primary data on expected lifetime, In addition, common end-of-life scenarios are not well known. Understanding various scenarios for end-of-life recycling, reuse, and disposal and the associated emissions of each scenario will enable more robust accounting of biogenic carbon storage and improve the overall life cycle modeling approaches for carbon-storing hempcrete.

5.0 Acknowledgments

This research was made possible by the Department of Civil, Environmental, and Architectural Engineering, the College of Engineering and Applied Sciences, the Living Materials Laboratory (LMLab), and the Discovery Learning Apprenticeship Program at the University of Colorado Boulder. This work represents the views of the authors and not necessarily those of the sponsors.

6.0 References

Adams, M., Burrows, V., Richardson, S., 2019. Bringing embodied carbon upfront. World Green Building Council, London, UK.

Arrigoni, A., Pelosato, R., Melià, P., Ruggieri, G., Sabbadini, S., Dotelli, G., 2017. Life cycle assessment of natural building materials: the role of carbonation, mixture components and transport in the environmental impacts of hempcrete blocks. Journal of Cleaner Production 149, 1051–1061. https://doi.org/10.1016/j.jclepro.2017.02.161

ASTM C150, 2019. C150M-19a Standard Specification for Portland Cement. ASTM International, West Conshohocken, PA.

Badogiannis, E., Kakali, G., Dimopoulou, G., Chaniotakis, E., Tsivilis, S., 2005. Metakaolin as a main cement constituent. Exploitation of poor Greek kaolins. Cement and Concrete Composites 27, 197–203. https://doi.org/10.1016/j.cemconcomp.2004.02.007

Boutin, M., Flamin, C., Quinton, S., Gosse, G., 2006. Etude des caractéristiques environnementales du chanvre par l'analyse de son cycle de vie. Ministère de l'agriculture et de la pêche MAP 4, B1.

Boutin, M.-P., Flamin, C., 2013. Examination of the Environmental Characteristics of a Banked Hempcrete Wall on a Wooden Skeleton, by Lifecycle Analysis: Feedback on the LCA Experiment from 2005, in: Amziane, S., Arnaud, L., Challamel, N. (Eds.), Bio-Aggregate-Based Building Materials. John Wiley & Sons, Inc., Hoboken, NJ 07030 USA, pp. 289–312. https://doi.org/10.1002/9781118576809.ch9

Breton, C., Blanchet, P., Amor, B., Beauregard, R., Chang, W.-S., 2018. Assessing the Climate Change Impacts of Biogenic Carbon in Buildings: A Critical Review of Two Main Dynamic Approaches. Sustainability 10, 2020. https://doi.org/10.3390/su10062020

Chabannes, M., Garcia-Diaz, E., Clerc, L., Bénézet, J.-C., 2015. Studying the hardening and mechanical performances of rice husk and hemp-based building materials cured under natural and accelerated carbonation. Construction and Building Materials 94, 105–115. https://doi.org/10.1016/j.conbuildmat.2015.06.032

Chabannes, M., Garcia-Diaz, E., Clerc, L., Bénézet, J.-C., Becquart, F., 2018. Lime Hemp and Rice Husk-Based Concretes for Building Envelopes, SpringerBriefs in Molecular Science. Springer International Publishing, Cham. https://doi.org/10.1007/978-3-319-67660-9

Collet, F., Pretot, S., 2014. Thermal conductivity of hemp concretes: Variation with formulation, density and water content. Construction and Building Materials 65, 612–619. https://doi.org/10.1016/j.conbuildmat.2014.05.039

Das, S., Souliman, B., Stone, D., Neithalath, N., 2014. Synthesis and Properties of a Novel Structural Binder Utilizing the Chemistry of Iron Carbonation. ACS Appl. Mater. Interfaces 6, 8295–8304. https://doi.org/10.1021/am5011145

Despotou, E., Shtiza, A., Schlegel, T., Verhelst, F., 2016. Literature study on the rate and mechanism of carbonation of lime in mortars / Literaturstudie über Mechanismus und Grad der Karbonatisierung von Kalkhydrat im Mörtel: Literature study on the rate and mechanism of carbonation of lime in mortars / Literaturstudie über Mechanismus und Grad der Karbonatisierung von Kalk. Mauerwerk 20, 124–137. https://doi.org/10.1002/dama.201500674

Dunstan, E.R., 2011. How does pozzolanic reaction make concrete "Green"? 2011 World of Coal Ash (WOCA) Conference 1–14. https://doi.org/10.1680/coma.2011.164.6.315

Ellingboe, E., Arehart, J., Srubar, W., 2019. On the Theoretical CO2 Sequestration Potential of Pervious Concrete. Infrastructures 4, 12. https://doi.org/10.3390/infrastructures4010012

EN, 2011. 15804: 2011.

Florentin, Y., Pearlmutter, D., Givoni, B., Gal, E., 2017. A life-cycle energy and carbon analysis of hemp-lime bio-composite building materials. Energy and Buildings 156, 293–305. https://doi.org/10.1016/j.enbuild.2017.09.097

Franklin Associates, 2009. Life Cycle Assessment of Drinking Water Systems (No. 09-LQ-104). State of Oregon Deparment of Environmental Quality.

Grist, E.R., Paine, K.A., Heath, A., Norman, J., Pinder, H., 2015. The environmental credentials of hydraulic lime-pozzolan concretes. Journal of Cleaner Production 93, 26–37. https://doi.org/10.1016/j.jclepro.2015.01.047

Hansen, J., Sato, M., Kharecha, P., von Schuckmann, K., Beerling, D.J., Cao, J., Marcott, S., Masson-Delmotte, V., Prather, M.J., Rohling, E.J., Shakun, J., Smith, P., Lacis, A., Russell, G., Ruedy, R., 2017. Young people's burden: requirement of negative CO2 emissions. Earth Syst. Dynam. 8, 577–616. https://doi.org/10.5194/esd-8-577-2017

Heath, A., Paine, K., McManus, M., 2014. Minimising the global warming potential of clay based geopolymers. Journal of Cleaner Production 78, 75–83. https://doi.org/10.1016/j.jclepro.2014.04.046

IECC, 2017. 2018 - International Energy Conservation Code.

Ip, K., Miller, A., 2012. Life cycle greenhouse gas emissions of hemp–lime wall constructions in the UK. Resources, Conservation and Recycling 69, 1–9. https://doi.org/10.1016/j.resconrec.2012.09.001

ISO, 2006a. ISO 14040: 2006 environmental management—life cycle assessment—principles and framework.

ISO, 2006b. ISO 14044: 2006-Environmental management-Life cycle assessment-Requirements and guidelines.

Johannesson, B., Utgenannt, P., 2001. Microstructural changes caused by carbonation of cement mortar. Cement and Concrete Research 31, 925–931. https://doi.org/10.1016/S0008-8846(01)00498-7

Jones, C., Hammond, G., 2019. Inventory of Carbon & Energy V3.0 Beta.

Khatib, J.M., Wild, S., 1996. Pore size distribution of metakaolin paste. Cement and Concrete Research 26, 1545–1553. https://doi.org/10.1016/0008-8846(96)00147-0

Lagerblad, B., 2006. Carbon dioxide uptake during concrete life cycle - State of the art (No. 03018). Swedish Cement and Concrete Research Institute, CBI.

Levasseur, A., Lesage, P., Margni, M., Samson, R., 2013. Biogenic Carbon and Temporary Storage Addressed with Dynamic Life Cycle Assessment. Journal of Industrial Ecology 17, 117–128. https://doi.org/10.1111/j.1530-9290.2012.00503.x

Magwood, C., 2016. Essential hempcrete construction: the complete step-by-step guide.

Mehta, P.K., 1986. Concrete. Structure, properties and materials. Prentice-Hall Incorporated, Englewood Cliffs, NJ.

Morandeau, A., Thiéry, M., Dangla, P., 2014. Investigation of the carbonation mechanism of CH and C-S-H in terms of kinetics, microstructure changes and moisture properties. Cement and Concrete Research 56, 153–170. https://doi.org/10.1016/j.cemconres.2013.11.015

Nonat, A., 2004. The structure and stoichiometry of C-S-H. Cement and Concrete Research 34, 1521–1528. https://doi.org/10.1016/j.cemconres.2004.04.035

Nordby, A.S., Shea, A.D., 2013. Building Materials in the Operational Phase: Impacts of Direct Carbon Exchanges and Hygrothermal Effects. Journal of Industrial Ecology n/a-n/a. https://doi.org/10.1111/jiec.12046

Ochoa George, P.A., Gutiérrez, A.S., Cogollos Martínez, J.B., Vandecasteele, C., 2010. Cleaner production in a small lime factory by means of process control. Journal of Cleaner Production 18, 1171–1176. https://doi.org/10.1016/j.jclepro.2010.03.019

Olajire, A.A., 2013. A review of mineral carbonation technology in sequestration of CO2. Journal of Petroleum Science and Engineering 109, 364–392. https://doi.org/10.1016/j.petrol.2013.03.013

Pittau, F., Krause, F., Lumia, G., Habert, G., 2018. Fast-growing bio-based materials as an opportunity for storing carbon in exterior walls. Building and Environment 129, 117–129. https://doi.org/10.1016/j.buildenv.2017.12.006

Pretot, S., Collet, F., Garnier, C., 2014. Life cycle assessment of a hemp concrete wall: Impact of thickness and coating. Building and Environment 72, 223–231. https://doi.org/10.1016/j.buildenv.2013.11.010

Souto-Martinez, A., Arehart, J.H., Srubar, W.V., 2018. Cradle-to-gate CO2e emissions vs. in situ CO2 sequestration of structural concrete elements. Energy and Buildings 167, 301–311. https://doi.org/10.1016/j.enbuild.2018.02.042

Souto-Martinez, A., Delesky, E.A., Foster, K.E.O., Srubar, W. V., 2017. A mathematical model for predicting the carbon sequestration potential of ordinary portland cement (OPC) concrete. Construction and Building Materials 147, 417–427. https://doi.org/10.1016/j.conbuildmat.2017.04.133

UNFCCC, V., 2015. Adoption of the Paris agreement. United Nations Office at Geneva, Geneva.

Walker, R., Pavía, S., 2014. Moisture transfer and thermal properties of hemp–lime concretes. Construction and Building Materials 64, 270–276. https://doi.org/10.1016/j.conbuildmat.2014.04.081

Walker, R., Pavia, S., Mitchell, R., 2014. Mechanical properties and durability of hemp-lime concretes. Construction and Building Materials 61, 340–348. https://doi.org/10.1016/j.conbuildmat.2014.02.065

Wild, S., Khatib, J.M., 1997. Portlandite consumption in metakaolin cement pastes and mortars. Cement and Concrete Research 27, 137–146. https://doi.org/10.1016/S0008-8846(96)00187-1

Wu, B., Ye, G., 2016. Carbonation Mechanism of Different Kinds of C-S-H: Rate and Products. Presented at the International RILEM Conference on Materials, Systems and Structures in Civil Engineering, Lyngby Denmark, p. 10.

Zampori, L., Dotelli, G., Vernelli, V., 2013. Life Cycle Assessment of Hemp Cultivation and Use of Hemp-Based Thermal Insulator Materials in Buildings. Environ. Sci. Technol. 47, 7413–7420. https://doi.org/10.1021/es401326a